FEATURE ARTICLE

Quantitative Prediction of Fluorescence Quantum Yields for Tryptophan in Proteins

Patrik R. Callis* and Tiqing Liu

Department of Chemistry and Biochemistry, Montana State University, Bozeman, Montana 59717

Received: September 9, 2003; In Final Form: December 31, 2003

Variation of intrinsic tryptophan (Trp) fluorescence intensity and lifetime in proteins is widely exploited to follow changes in protein structure such as folding/unfolding, substrate or ligand binding, and protein−protein interactions. Although a credible candidate for the source of weak Trp fluorescence in some proteins has long been believed to be electron transfer from excited Trp to an amide carbonyl group, recognition of when such a process should be exceptionally efficient has not been possible. Here we propose a reasonable basis for the 30-fold variation by the use of quantum mechanics−molecular mechanics simulations in which the energy of the lowest Trp ring-to-amide backbone charge transfer (CT) state is monitored during dynamics trajectories for 24 Trps in 17 proteins. The energy, fluctuations, and relaxation of high lying CT states are extremely sensitive to protein environment (local electric field direction and strength). Application of basic electron transfer theory with a single empirical electronic coupling reveals that the entire 30-fold range is explainable from local electric field effects on electron transfer to a nearby amide, although other acceptors may sometimes be responsible for a low yield. A key new concept uncovered in this work is that charged groups near the Trp can have profound effects on fluorescence lifetime and quantum yield, but location is critical. Negative (positive) charge will decrease (increase) quantum yield if closer to the indole ring than to the electron acceptor because these arrangements stabilize (destabilize) the CT state. If the charge is closer to the acceptor, the opposite will be true. A semiquantitative prediction using only the average energy gap and variance was achieved by using a universal electronic coupling constant and energy offset.

Introduction

One of the most intriguing questions related to the widely used intrinsic fluorescence of tryptophan (Trp) in proteins is the extreme variation of fluorescence quantum yields (Φ_f) and lifetimes in different protein environments. The yields vary from near 0.35 down to 0.01 or less.[1] This is particularly interesting because the light-absorbing part of Trp, effectively 3-methylindole (3MI), shows little variability in Φ_f when dissolved in different solvents varying in polarity from pure hydrocarbon to water, being always near 0.3.[2] Even without being understood, the strong sensitivity of Trp fluorescence intensity to microenvironment is routinely exploited to follow a variety of protein changes, e.g., ligand/substrate binding and folding/unfolding.[1,3−7]

Although there has been considerable interest in understanding these variations, no convincing detailed mechanism has emerged. Whereas proton transfer from the ammonium group is implicated in reducing Φ_f for free Trp in solution at pH < 9,[8−13] compelling evidence accumulated over some time supports a mechanism involving electron transfer from the excited indole ring for the low Φ_f in proteins (where the ammonium and carboxylate groups of the free Trp become amides).[13−21] Whereas for proteins the identity of the electron acceptor group(s) was almost always in question, the universal loss of fluorescence quantum yield found for a variety of small Trp derivatives containing an amide group clearly implicated the amide group as an acceptor.[11,19,22−25]

The Barkley group has made extensive investigations into the collisional quenching of 3MI fluorescence by *acylated* amino acids (to avoid interference from proton transfer quenching) in solution. In addition to strongly quenching groups such as disulfide, protonated histidine, carboxylic acids, and thiols, electron-transfer quenching by amides in aqueous solution was also demonstrated,[13,16] provided that two or more amide groups are in close proximity. A number of recent works have invoked electron-transfer quenching by the local peptide carbonyl group in their explanation of fluorescence lifetime data.[26−30]

N-Acetyltryptophanamide (NATA, see Figure 1), whose only potential quenching mechanism would appear to be electron transfer to an amide group, serves as an icon in this respect. Φ_f of 3MI in water is 0.34 compared to 0.14 for NATA.[11,12] The fluorescence lifetimes of both are single-exponential with NATA showing about a 3-fold reduction in lifetime compared to 3MI.[11,12]

A difficulty in accepting a local amide as the acceptor has been that amides are not good electron acceptors. In addition, there has been difficulty seeing how such wide variation in Φ_f can arise; every Trp in any protein has several nearby amide groups, so why is the fluorescence for Trps in certain proteins, e.g., azurin, ribonuclease T1, and Staph. nuclease, not quenched at all?

Previous attempts to make quantitative correlations of Trp fluorescence lifetimes and quantum yields to electron transfer have been fragmentary[26−30] and appear to be influenced by the large body of recent work on long-range electron transfer in

* To whom correspondence should be addressed. Phone: 406-994-5414. Fax: 406-994-5407. E-mail: pcallis@montana.edu.
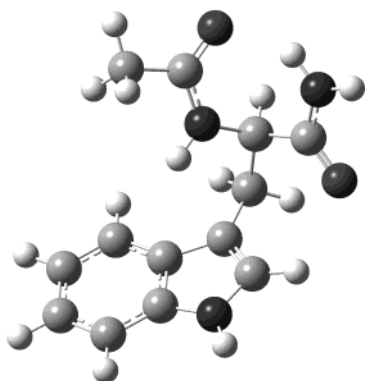
Feature Article

J. Phys. Chem. B, Vol. 108, No. 14, 2004 **4249**

Figure 1. Structure of *N*-acetyltryptophanamide (NATA). All quantum calculations (INDO/S2−SCI) were done on *N*-formyltryptophanamide (NFTA), which differs from NATA by replacement of the methyl of the acetyl group by a hydrogen. Geometry and electrical potentials from the protein environment were determined using Charmm.

proteins, where much attention is paid to the electronic coupling and its exponential dependence on donor−acceptor distance.[31−33] Recent works attributing Trp quenching to amide groups at short range have assumed that the electron transfer rate decreases exponentially with the donor−acceptor distance but have typically not been able to make reasonable estimates of the equally (or more) important parameters associated with the activation energy (reorganization energy and free energy change, including electrostatic stabilization). In this paper, we try to be comprehensive, recognizing that for short-range electron transfer the electronic coupling is quite strong and, therefore, is unlikely to be the rate-limiting variable. Instead, we emphasize the crucial point in Marcus theory that electron transfer can compete with (quench) fluorescence only if the *local electric field and/or solvation energy* tunes the fluorescing state (^1L_a) into resonance with a Franck−Condon accessible vibrational level of the resulting charge transfer (CT) state.[34−36] The original Marcus view is taken, i.e., that electron transfer is simply a radiationless electronic transition, in this case internal conversion between the usual lowest excited state and a high-lying CT vibronic state that is momentarily stabilized by a solvent and/or geometry fluctuation such that the two states have the same *energy*.[34−37]

The work presented here is an extension of our recent successful application of a custom hybrid quantum mechanical−molecular mechanics (QM−MM) method to the prediction of Trp fluorescence wavelength shifts due to protein electric fields and solvation,[38,39] except that it is applied to assessing the energy gap between solvent-relaxed ^1L_a and the lowest lying CT excited-state instead of predicting the energy gap between solvent-relaxed ^1L_a and the ground state. As with the latter, an important aspect is assessing stabilization of the weakly emitting CT state by environmental response after formation (reorganization energy). We will contend that without rapid, large-amplitude relaxation of the CT state, recombination of the separated charges (return to the ^1L_a state) will nullify quenching. A preliminary report of these results has recently appeared.[40]

Methods

We use a generalization of our hybrid QM−MM method used recently to predict the fluorescence wavelengths of Trp in proteins,[38] wherein the QM part is Zerner's INDO/S-CIS method,[41] as modified to include the local electric field and potentials.[42,43] A particularly critical modification was modification to INDO/S2 by inclusion of a more appropriate set of parameters for oxygen suggested by Li et al.[44] The MM part is Charmm (version 26b).[45] In contrast to our wavelength

prediction study,[38] the QM part is not restricted to the indole ring plus CB of Trp but now includes the Trp amide and that of the preceding residue. These are capped with hydrogens so that the QM part is *N*-formyltryptophanamide (NFTA; see Figure 1). Other significant expansions of the method are that the geometry for the QM molecule is dictated by the MM, allowing the discovery of critical geometries that may stabilize the CT complex, and the atom charges are determined from the total electron density instead of just changes in π density. New carbon atom types were added to the Charmm topology and parameter files so that geometries specific to the ^1L_a and CT excited states were selectable via the protein structure file. The bond lengths and angles were assigned as found from CIS/3-21G calculations. For the runs reported in this work, the bond lengths of the QM part were kept constant at values corresponding to the CT state using the shake command.[46] We have resorted to a trick of putting *all* amide groups in the CT geometry as well as the indole ring, even though only one amide at a time would have this geometry. The reason for this procedure is to avoid the enormous amount of extra work required to examine multiple trajectories wherein a different amide was in the CT geometry. The effect of forcing all of the amides into the CT geometry is primarily to add a constant energy to each state and should not significantly affect energy differences.

The method is further extended to deal with pairs of amino acid residues, wherein one member is the aforementioned *N*-formyltryptophanamide and the other is the *N*-formyl amide of any other chosen residue of the protein. The pair is then treated as a single molecule (supermolecule).

Among the excited singlet states are charge transfer (CT) states that may be described as resulting from the excitation of an electron from a donor molecular orbital (MO) to an empty MO on the acceptor, creating a "radical ion pair". We note that the supermolecule approach automatically includes the Coulombic interaction of the "radical pair" and relaxations about these charges. This has been left out of many analyses in the literature.

Identifying the lowest CT state is nontrivial because of the fluctuating external fields and geometry (taken from the MM). Ideally, one would simply look for the lowest state whose integrated charge on the indole rings is ∼+1. However, for any given point in a trajectory, this state is often mixed with other states. Instead of choosing an arbitrary threshold of the ring charge for defining the CT state, we have adopted a procedure that reports the lowest CT state energy as the ring-charge-weighted average energy of those states comprising the lowest CT mixed states, identified as having a net positive charge on the indole ring + CB methylene group and the sum of which is +1. The software will detect CT states for which the indole ring is the electron acceptor, but such states have not emerged as important to this point in our studies.

Franck−Condon factors associated with the ^1L_a − CT coupling matrix element were computed following the method we used in several recent studies.[47−49] However, in this case, a direct product space was established for the two independent systems, indole and formamide. The geometry change for the indole was the difference for indole in the ^1L_a state minimum from a geometry optimization at the CIS/3-21G level and the indole part of a coplanar indole-formamide sandwich dimer (separation = 4.5 Å) in its lowest CT state, also optimized at CIS/3-21G. For formamide, the geometry difference came from the ground-state HF/3-21G and the same optimized CT geometry as for indole. The vibrational frequencies and modes used were

TABLE 1: Excitation Energies (in 1000 cm⁻¹) for Indole−Amide Coplanar Sandwich Dimer (4.5 Å Spacing) Comparing Zindo, TDDFT, and CASPT2 Transition Energies at Different Geometries

state:	L_a				L_b				CT		
geometry	CASPT2	TDDFT	Zindo	expt.	CASPT2	TDDFT	Zindo	expt.	CASPT2	TDDFT	Zindo
CT[a]	35.27	36.45	34.77		31.95	39.88	33.11		51.10	33.82	44.41
La[b]	35.03	35.76	34.53	34.5[d]	30.92	38.94	32.65		61.28	43.59	53.36
ground[c]	39.13	39.60	38.99	38.9[e]	32.44	40.86	34.30	35.2[f]	64.82	46.68	57.03

[a] Charge transfer (CT) geometry. [b] ¹La geometry. [c] Ground-state geometry; CT and ¹La are optimized with CIS/3-21G; ground state is optimized with HF/3-21G. [d] Estimated from ¹La origin in cold jet[61] and width of gas-phase absorption.[67] [e] Gas-phase absorption maximum.[67] [f] ¹Lb origin in cold jet.[68]

those for the neutral ground-state molecules, determined at the B3LYP/6-311G(d,p) level. Bond length parameters for histidine, the histidine radical anion, protonated histidine, and the protonated histidine neutral radical were determined from HF/6-311G(d,p) geometry optimizations on 4-methylimidazole and are considered provisional at present.

Time dependent density functional (TDDFT) calculations of transition energies were also performed at the B3LYP/6−311G(d,p) level. Geometry optimizations, CIS, and TDDFT calculations were performed using Gaussian 98, Rev. A11.3.[50]

Complete active space self-consistent field (CASSCF) calculations and their second order perturbation extension (CASPT2) were done using MOLCAS5.4[51] with an atomic natural orbital type basis set contracted to C,N,O 3s2p1d/H 2s. To find the high-lying CT energy using the CASPT2 method required state averaging over the lowest 18 eigenstates in a vacuum. Level shifting was necessary for precisely locating the energies.

Results

Nature of the Charge Transfer State. The electronic structure of the indole ring and of the amide chromophore have been individually studied at the highest theoretical levels available.[52,53] For many years, the nature of the fluorescing state of Trp in proteins was rather uncertain because of the accidental degeneracy of the two lowest singlet $\pi\pi^*$ states, labeled ¹La and ¹Lb.[54,55] More recently, polarized one- and two-photon spectra of several indoles in solution,[56−58] in cold jets,[59,60] and in solid argon[61,62] have provided confidence that the fluorescing state of Trp in proteins is the solvent-sensitive ¹La,[63] with the possible exception of Trp48 of azurin, for which ¹La and ¹Lb appear to be quite close in energy. QM−MM simulations[38,39,64−66] and detailed calculations of vibronic band shapes[47−49] have provided harmonious support to these experiments.

The focus of this study, however, is on a state (herein called CT) involving an intramolecular electron transfer between these two systems, for which there seems to be neither direct experimental evidence nor theoretical investigation. Whereas Zindo is known to be well calibrated for heteroaromatic $\pi\pi^*$ transitions, its accuracy for the CT transition of interest here is unknown. In the absence of experimental information, we rely on two ab initio methods, TDDFT/B3LYP and CASPT2, to help assess the accuracy of the Zindo method for a model system. Table 1 compares the ¹La, ¹Lb, and CT transition energies found for a model indole−formamide coplanar sandwich dimer with 4.5 Å interplanar spacing using Zindo, TDDFT/B3LYP, and CASPT2 at optimized geometries for the ground, ¹La, and CT states in a vacuum. The CT state in this system is well described by a single configuration involving promotion of an electron from the HOMO of the indole ring to the LUMO of the amide, illustrated in Figure 2. For more realistic systems such as NFTA and NATA, the CT state is typically somewhat mixed with other configurations but usually dominated by this configuration. The presence of the amide has little effect on the computed ¹La and
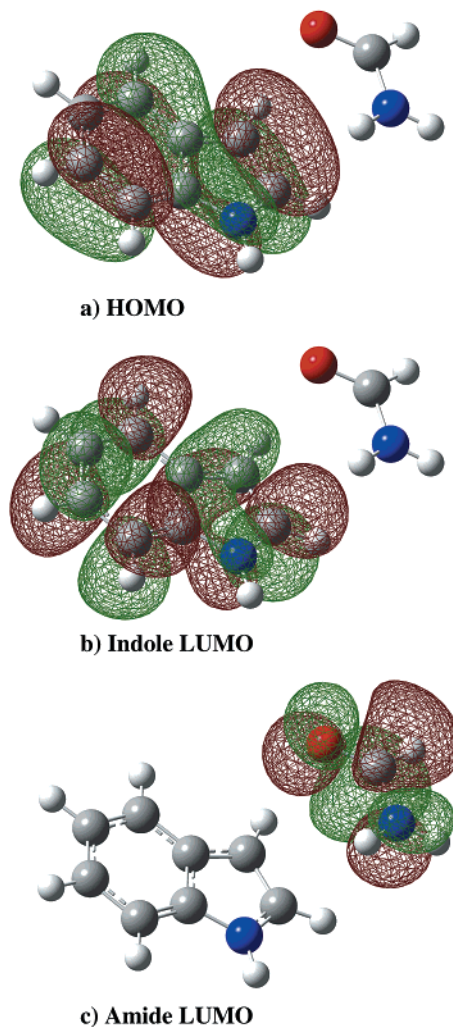

a) HOMO

b) Indole LUMO

c) Amide LUMO

Figure 2. Structure and key molecular orbitals involved in the ¹La and CT states of an indole-formamide sandwich complex with 4.5 Å spacing. (a) Highest occupied molecular orbital (HOMO) of indole; (b) Lowest unoccupied MO (LUMO) of indole; (c) LUMO of formamide. The latter is a pi* MO highly localized at the C, but with substantial antibonding character in the CO and CN bonds. The ground → ¹La transition is primarily described by the HOMO−LUMO transition on indole, but with minor contributions from other configurations. The ground → CT transition is well described by the single configuration resulting from promotion of an electron from the indole HOMO to the amide LUMO. The MOs in this figure were plotted from a HF/6-311G(d,p) calculation using GaussView98, but visually were indistinguishable from those using the 3-21G basis. The general features were the same as found from the Zindo calculations used for the QM−MM simulations.

¹Lb transition energies. Experimental values are included when available. For the ground-state geometry, appropriate experimental values are the vapor absorption maxima, taken from Strickland et al.[67] for ¹La and from Bickel et al.[68] for ¹Lb. For the ¹La geometry, we estimate the vertical transition energy to

Feature Article

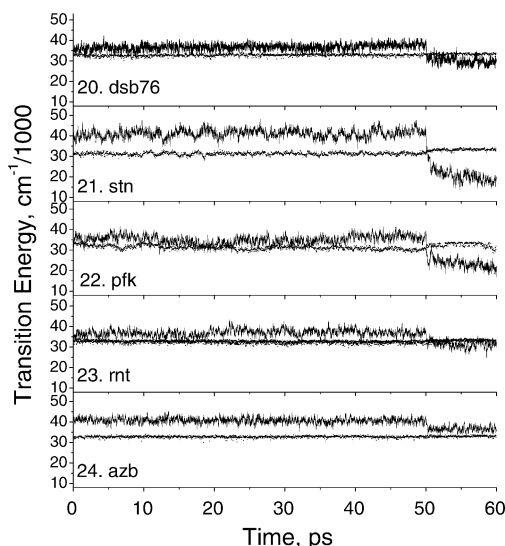*J. Phys. Chem. B, Vol. 108, No. 14, 2004* **4251**

Figure 3. Vertical transition energy, $\Delta E/1000hc$ for the ground $\rightarrow$ ^1L_a state (dots) and the ground $\rightarrow$ lowest Trp ring-amide charge transfer (CT) state transitions (line) during a 60 ps QM−MM trajectory for high quantum yield (quantum yields 0.2−0.3) tryptophans (Trps). The bond lengths (but not angles and torsions) were held constant at values corresponding to the CT state (see Methods section). During the first 50 ps the charges on the Trp are those of the ^1L_a state (scaled by 0.80) and are updated every 10 fs. During the last 10 ps the charges are those of the CT state. Note the much greater fluctuation amplitude for the CT state than for ^1L_a.

Figure 4. Same as Figure 3, except for Trps with quantum yield between 0.06 and 0.15.

the ground state from the location of the ^1L_a origin in a cold beam[61] and subtract the estimated width obtained from the gas-phase absorption.[67] For ^1L_a, mutual agreement is good (within 1000 cm^{-1}, 0.1 eV) for all three methods at all three geometries, including with the experimental values. For ^1L_b, which is S_1 in a vacuum and nonpolar solvents, Zindo and CASPT2 again agree well with experiment, but TDDFT is systematically about 1 eV high. For the CT case, where no experimental information is available, at all three geometries Zindo is about 1 eV below CASPT2 but about 2 eV above TDDFT. Whereas TDDFT is often a reliable method for predicting transition energies, at least one other case has documented its tendency to greatly under-estimate the energy of CT transitions relative to the more reliable CASPT2 method.[69]

That the Zindo and CASPT2 CT energies lie far above that of ^1L_a in a vacuum seems clear. In our QM−MM calculations, solvent polarization by the system when in the ^1L_a state considerably lowers the CT energy relative to ^1L_a, and in certain protein environments the local electric field is so strong that the two states are very close in energy. Although it appears that Zindo may appreciably underestimate the CT energy, we have checked the variation of the CT energy in a strong electric field and find that the energy change with field is very similar for Zindo and CASPT2. This means that the large fluctuations in CT energy given by Zindo during MD simulations should be reasonably accurate if the fields derived from Charmm are accurate.

Our early results for the histidine cation quenching indicate that the electron is added to a pi* MO localized on the ND-CE-NE fragment and is strongly antibonding in both bonds. For either the HF/3-21G or the HF/6-311G(d,p) basis set, these two bond lengths increase by about 0.1 Å. The nature of the orbital is quite similar to the electron-accepting antibonding MO on the amide groups, for which similar bond length increases are computed.
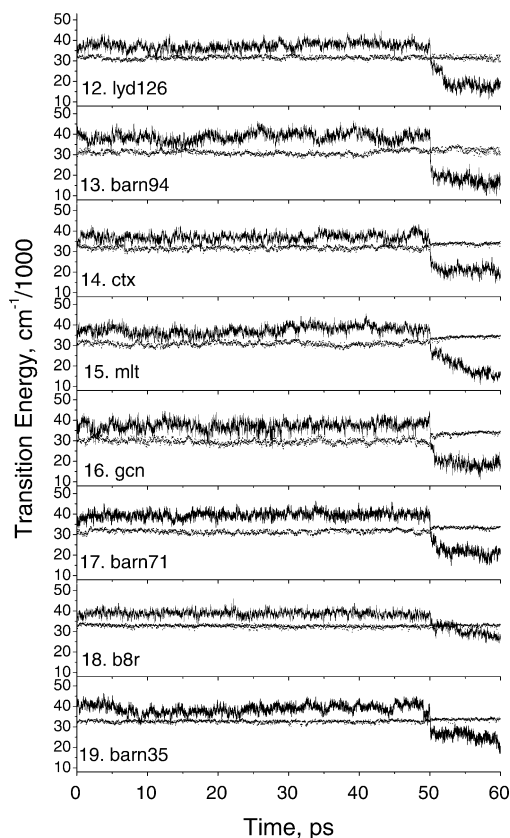
QM−MM Trajectories. Figures 3−5 display the ground $\rightarrow$ lowest CT and ground $\rightarrow$ ^1L_a INDO/S2−CIS computed vertical transition energies during 60 ps dynamics trajectories for 24 Trps in 17 different protein environments. The geometry used for these trajectories is that of the CT state (see Methods and Table 1). The energies are relative to the ground electronic state also in the CT geometry. During the first 50 ps, the Trp charge distribution is that of the ^1L_a state, but during the last 10 ps, the charges are those for the lowest CT state for which an electron has been transferred from the indole ring to one of the two backbone amide groups on the Trp or to one of the two amides or side chain of another residue. This part of the trajectories always shows relaxation of the CT energy due to solvent and side chain response to the considerably different charge distribution in the CT state. Quenching occurs if this relaxation brings the poorly emitting CT state irreversibly below the ^1L_a state.

Figures 2−4 divide the results for three groups that can be regarded as Trps having high, intermediate, and low fluorescence quantum yields, respectively. Figure 3 displays results for Trp48 of azurin, Trp140 of Staph. nuclease, Trp59 of ribonuclease T1, Trp179 of Pfk, and Trp76 of DsbA for which the observed Φ_f values are high (0.2−0.3), corresponding to small or negligible electron transfer quenching. Figure 5 collects similar results for Trps exhibiting exceptionally low Φ_f (<0.01 to 0.05), and Figure 4 shows those with intermediate Φ_f values (0.06−0.15).

Surprising features of these trajectories are the extremely high amplitude, high-frequency fluctuations of the CT state energy relative to those of ^1L_a and the concomitant large amplitude, fast relaxations of this state following the simulated electron transfer. Three properties of the trajectories are crucial to the fluorescence quantum yield: (1) the average energy gap separating the CT and ^1L_a states, (2) the amplitude of fluctua-

4252 *J. Phys. Chem. B, Vol. 108, No. 14, 2004*

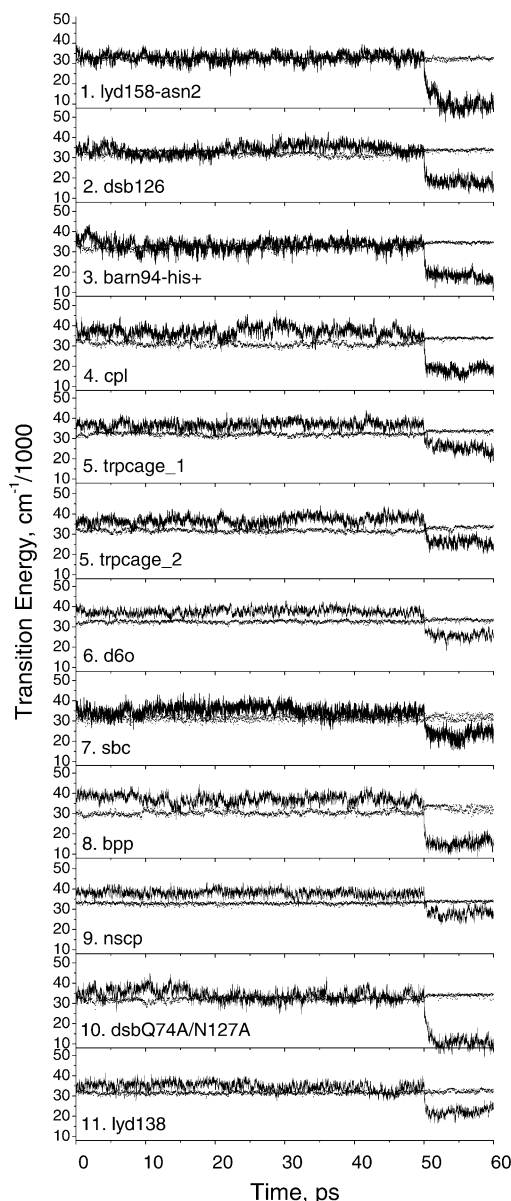Fluorescence Quantum Yields for Trp in Proteins

Figure 5. Same as Figure 3, except for Trps with quantum yield between 0.01 and 0.05.

tions of this energy gap, and (3) the rapidity and extent of relaxation following an electron-transfer event. The first two affect the probability of a CT−^1L_a crossing, a necessary condition for electron transfer. The third determines whether the fluorescence will be permanently quenched because the weakly emitting CT state is stabilized far enough below the ^1L_a state that back transfer is prevented. The latter is related to the second,[70] and we find here, as has been well established for smaller solutes in water,[71] and through simulations on 3MI,[64] that much relaxation occurs within tens of femtoseconds when the Trp is exposed to fluid water.

The set of limited trajectories contained in Figures 3−5 reveals a remarkable variety of behaviors in the three properties just listed. In a broad sense, there is correlation of these properties with observed quantum yields, although there are notable exceptions. The most important aspect of this variety is that a clear source of the wide variation in quantum yields presents itself.

The origin of the large fluctuations and difference in average gap can be traced to the local electric field (potential difference) caused not only by the intermolecular electrostatic interactions,
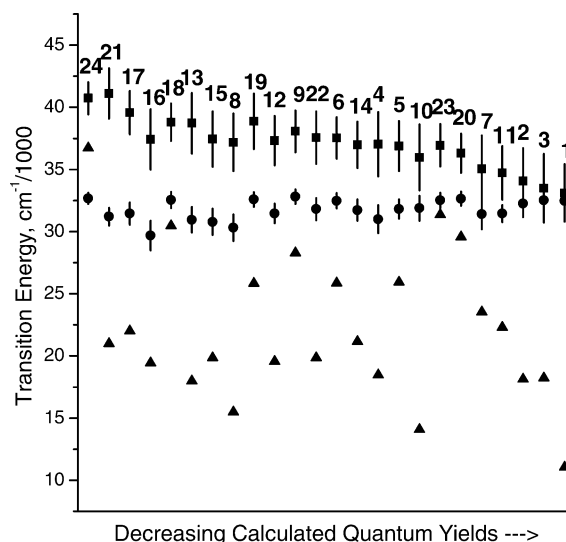

Figure 6. Condensation of data from QM−MM trajectories for 24 Trps from 17 proteins in order of decreasing Trp calculated fluorescence quantum yield. Solid squares: average CT energy with standard deviation given by half of the vertical line. Solid circles: average ^1L_a energy with standard deviation given by half of the vertical line. Triangles: average energy of the relaxed CT state, from the last 10 ps of the trajectory. The labels refer to the number code shown in Table 2.

but also by intramolecular differences in the Coulombic energy of the separated charges for slight changes in amide-ring separation and orientation. Upon investigating the microscopic description of the relaxation process, we find that most of the relaxation is caused by water reorientation.

Figure 6 summarizes the CT (top) and ^1L_a (middle) average transition energies, with their standard deviations indicated and the solvent relaxed CT transition energy (triangles) for the full set of 24 Trps in 17 proteins studied. The points are arrayed in order of decreasing calculated Φ_f, with the highest yield on the left. Note the correlation of increased quantum yield with increased CT−^1L_a gap. Some of the high quantum yield cases have relatively small gaps, but also show small relaxation.

Quantitative Estimates of Electron-Transfer Rates. The quantum mechanical Fermi Golden Rule expression for the transition rate from a well defined initial state to a continuum of final states nominally of the same energy is given by

$$\text{rate} = \frac{2\pi}{\hbar}|V_{el}|^2\rho(E) \tag{1}$$

where V_{el} is the electronic coupling between the initial and final states (assumed constant over the range of final states) and ρ-(E) is the density of final states in units of energy^{-1}.

The above expression applied to the electron-transfer rate constant of interest here is

$$k_{ET}(\Delta E_{00}) = \frac{2\pi}{\hbar}|V_{el}|^2\rho_{FC}(\Delta E_{00}) \tag{2}$$

where V_{el} is the (constant) electronic matrix element coupling the CT and ^1L_a states and $\rho_{FC}(\Delta E_{00})$ is the Franck−Condon-weighted density of final CT vibronic states that are quasi-degenerate with the initial state (^1L_a). $\rho_{FC}(\Delta E_{00})$ is a function of ΔE_{00}, the energy difference between of the vibrational zero points of the CT and ^1L_a states, $E_0(CT) − E_0(^1L_a)$ and is approximated by[72]

$$\rho_{FC}(\Delta E_{00}) = \int F_{D\rightarrow D+}(\Delta E_{00},E)F_{A\rightarrow A-}(\Delta E_{00},E)\, dE \tag{3}$$

Feature Article

J. Phys. Chem. B, Vol. 108, No. 14, 2004 **4253**

TABLE 2: Experimental and Calculated Fluorescence Quantum Yields for 24 Trps in 17 Proteins

expt.	calc.[a]	num	run/abreviation	description[b]	ref[c]
0.013	0.003	1	lyd158-asn2	T4 lysozyme W158-asn2 1lyd	111
0.013	0.005	2	dsb126	dsBa W126 1dsb	90
0.017	0.004	3	barn94-his18+	barnase W94−H18 pH5 1a2p	81
0.025	0.023	4	cpl	human cyclophilinA 2cpl	112
0.03	0.026	5	trpcage	TrpCage 1l2y (nmr structure 1&2)	7[d]
0.03	0.035	6	d6o	fkb506 binding protein 1d6o	113[e]
0.03	0.009	7	sbc	subtilisin C 1sbc	1[f]
0.031	0.047	8	bpp	phospholipase A2 2bpp	1
0.033	0.018	9	nscp	NSCP W57 W4F W170F	28
0.041	0.042	10	dsbQ74A/N127A	dsba W126 Q74A, N127A mutanted 1dsb	90
0.044	0.009	11	lyd138	T4 lysozyme W138 1lyd	111
0.06	0.047	12	lyd126	T4 lysozyme W126 1lyd	111
0.072	0.069	13	barn94	barnase W94 pH8 1a2p	81
0.1	0.030	14	ctx	cobra toxin 1ctx	1
0.115	0.058	15	mlt	melittin 2 mLt	1
0.12	0.080	16	gcn	glucagon 1gcn	1
0.122	0.225	17	barn71	barnase W71 his neutral 1a2p	81
0.13	0.121	18	b8r	parvalbumin 1b8r	1
0.142	0.048	19	barn35	barnase W35 his neutral 1a2p	81
0.2	0.014	20	dsb76	dsba W76 1dsb,1fvk average result	90
0.29	0.275	21	stn	staph. nuclease firstn	1
0.31	0.011	22	pfk	phosphofructokinase 6pfk	1
0.31	0.021	23	rnt	ribnuclease T1 9rnt	1
0.31	0.296	24	azb	apo-azurin W48 1azb	1

[a] From eq 4 using $|V_{el}| = 10.0$ cm^{-1}, $C_{00} = -4000$ cm^{-1}. [b] Name, Trp sequence number or Trp-acceptor numbers, PDB code (all X-ray unless noted). [c] Reference for experimental quantum yield. [d] Estimated relative to NATA. [e] Upper limit based on the 12-fold increase upon denaturation. [f] Estimated from lifetimes.

This is the overlap of the photoelectron spectrum of the indole ring with that of the acceptor anion. The isomorphic role of the FC-weighted density of states overlap for electron transfer and the more familiar Förster resonance excitation energy transfer (FRET)[73,74] was perhaps first emphasized by Hopfield.[72] In room temperature condensed phase, the plethora of low frequency vibrational modes associated with solvent and protein are typically treated classically.[37] In addition, these motions can drastically modify the relative energy of the ^1L_a and CT states, rapidly modulating the set of final states in resonance with the initial state. We assume that fluctuations in the environment modulate ΔE_{00} randomly and rapidly on the fluorescence lifetime scale, leading to a Gaussian distribution for ΔE_{00} and an average ET rate constant given by

$$\langle k_{ET} \rangle = 4\pi^2 c \langle |V_{el}^2| \rangle (2\pi\sigma^2)^{-1/2} \int \rho_{FC}(\Delta E_{00}) \times$$
$$\exp\left(-\frac{1}{2}\left(\frac{\Delta E_{00} - \overline{\Delta E_{00}}}{\sigma}\right)^2\right) d\Delta E_{00} \quad (4)$$

where all energies have been divided by hc so as to be expressed in cm^{-1}. Our approach follows the ideas of Hopfield[72] and Tachiya.[35] The notation $\langle |V_{el}^2| \rangle$, indicates that the electronic coupling is itself being modulated by the low-frequency motions, but that an effective average value can be used. The connection between eq 4 and the widely used high-temperature classical limit equation that has become almost synonymous with Marcus theory

$$k_{ET} = \left(\frac{4\pi^2}{h}\right) V^2 (4\pi\lambda k_B T)^{-1/2} \exp\left(-\frac{(\Delta G_0 + \lambda)^2}{4\lambda k_B T}\right) \quad (5)$$

is traced from the first quantum mechanical treatment of nonadiabatic electron transfer by Levich and Dogonadze through forms that recognize electron transfer as a case of radiationless electronic transition[75] in extensive reviews by Marcus and Sutin,[76] Bixon and Jortner,[37] and Tachiya and co-workers.[77] In
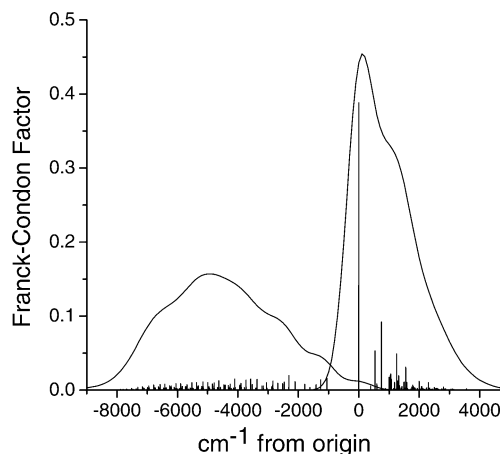

Figure 7. Ab initio computed Franck−Condon (FC) factors for the ionization of indole (right) and electron capture of formamide (left). The smooth curves of FC density were generated by broadening each line by 1000 cm^{-1}. The position of the curves is for $\Delta E_{00} = 0$, but protein electric fields that stabilize the indole ring cation and/or destabilize the amide anion will cause the curves to overlap. Furthermore, large (thousands of cm^{-1}) fluctuations of the CT−^1L_a gap caused by environmental motions shift the curves rapidly, thereby modulating the overlap (and therefore the coupling element) as a function of time.

eq 5, λ is the reorganization energy, k_B is the Boltzmann constant, and ΔG_0 is the difference in free energy of the equilibrium states. The amplitude of the fluctuations in ΔE_{00} determines the width of the Gaussian and is related to the reorganization energy by $\sigma^2 = 2\lambda k_B T$. The average CT−$^1L_a$ energy gap is closely related to $\Delta G_0 + \lambda$.

Figure 7 shows the ab initio computed functions $F_{D \rightarrow D+}$ and $F_{A \rightarrow A-}$, plotted so that $\Delta E_{00} = 0$. The donor and acceptor are indole and formamide. The continuous curves are obtained from the individual FC factors for the in-plane vibrations (shown as sticks) by applying a somewhat arbitrary 1000 cm^{-1} fwhm Gaussian line shape to each. The large relative geometry changes in the formamide bond lengths lead to an extremely broad band compared to the indole ring. The many thousands of closely
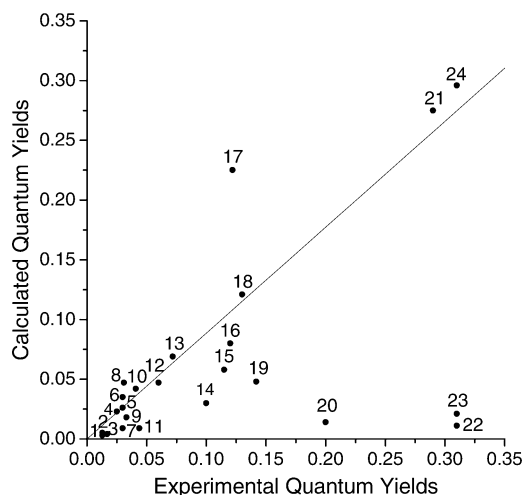
4254 *J. Phys. Chem. B, Vol. 108, No. 14, 2004*

Fluorescence Quantum Yields for Trp in Proteins

Figure 8. Plot of Trp fluorescence quantum yields calculated using eq 4 as a function of observed quantum yields for the set of Trps in Figure 6. The line represents a linear regression through zero for all points except for the three outlying point at the lower right and gives a correlation coefficient = 0.90. Observed quantum yields are referenced in Table 2 along with the number code.

spaced FC factors providing most of the area under the curve are invisible on the scale used in Figure 7.

Preliminary attempts to estimate values for V_{el} indicate that it is extremely sensitive to orientation of the ring and amide, much more so than assumed by Adams et al.[29] Our results were much as found by Stuchebrukhov and co-workers[78] for longer range coupling elements in proteins, wherein the magnitude varies from zero to maximum values on the time scale of tens of femtoseconds. Such a result might also be anticipated from the findings of Beratan et al.,[33] who found coupling between 33 non-H atoms at a distance $4-5$ Å from the heme in cytochrome *c* to be scattered randomly over two orders of magnitue (4 orders of magnitude in rate). We find that the value averaged over a trajectory is not sensitive to any measure of the distance between ring and amide for the restricted range of Trp ring-amide geometries found in the proteins studied, nor is it significantly different for different proteins. We expect that, for any given local geometry, V_{el} will be a complicated mixture of through bond and through space contributions.[31,33]

An additional major uncertainty is the value of the crucially important average energy gap, ΔE_{00}, as underscored by the discrepancy between the Zindo- and TDDFT-calculated values seen in Table 1. Given these uncertainties and the goal of this paper (more conceptual than quantitative) we use V_{el} and a constant offset, C_{00}, from the Zindo-calculated ΔE_{00}, as adjustable parameters to optimize a global fit with experiment, assuming that $|V_{el}|$ is the same for all cases. This is consistent with our view that V_{el} is not the rate-limiting factor.

Figure 8 shows computed Trp fluorescence quantum yields plotted against reported experimental quantum yields, calculated from the electron-transfer rate constants according to the relation

$$\Phi_f = k_r/(k_r + k_{nr} + k_{et})$$

where k_r and k_{nr} are the radiative and the nonelectron-transfer nonradiative rate constants. Here we use values found in aqueous solution: $k_r = 4 \times 10^7$ s^{-1} and $k_{nr} = 8 \times 10^7$ s^{-1}.[12] A more refined approach would be to recognize that both k_r and k_{nr} increase in nonpolar solvents,[2] in such a way that the quantum yield remains nearly constant. For the present analysis, we ignore this detail. The line in Figure 8 is a least-squares fit that excludes the three high quantum yield points with very low calculated

values, and is obtained using $|V_{el}| = 10$ cm^{-1} and $C_{00} = -4000$ cm^{-1}, providing a correlation coefficient equal to 0.90. This fit was selected from a basin of acceptable fits whose broad minimum was found at $|V_{el}| = 4.5$ cm^{-1} and $C_{00} = -5650$ cm^{-1} using a genetic algorithm. Despite the approximation of assuming constant V_{el}, the fit captures the known variability of Φ_f in a way that generally agrees with experiment, with a few egregious disagreements that we discuss next.

The most obvious disagreements occur for three systems that show quite high quantum yields, namely rnt, pfk, and W76 of dsba. The special feature underlying these cases is the small gap but also a small reorganization energy. We believe that the small reorganization energy is a significant indicator of high quantum yield but that our theoretical parametrization is weighted in such a way as to force the relaxed state slightly below ^1L_a (see Figure 6). This, along with the small gap makes the computed quantum yield low. Had the relaxed CT energy been only 2.8 kcal/mol (700 cm^{-1}) above ^1L_a, one would estimate a quantum yield of 0.3 for these cases from the Boltzmann equilibrium ratio of CT to ^1L_a population.

Intermolecular Electron-Transfer Quenching. The focus of this paper is primarily upon the local ring-amide CT states, because the results suggest that they are mainly responsible for the quenching process. However, the possibility that nearby amides belonging to other residues and histidines may contribute was also investigated for the obvious near neighbor cases. A search for Trps with asparagines and glutamine amide groups within about 4 Å turned up Asn6 of bpp, Asn117 of sbc, Gln105 of lydW138, and Asn2 of lydW158. For these, separate trajectories were run wherein the QM part was a supermolecule of the Trp and the nearby residue of interest. For the first three of the four cases examined, the lowest CT state was found on the non-Trp side chain amide only $4-10\%$ of the time, and had little effect on the computed quantum yield. However, for Asn2 of lydW158, the lowest CT state was found on the N-terminal amide of the Asn2 (actually the carbonyl of Met1, the N-terminus of the protein) virtually 100% of the time and lowered the predicted quantum yield from 0.07 to 0.013, greatly improving agreement with experiment. The reason is that the CT state is stabilized by the positive charge of the N-terminus, which is closer to the carbonyl than to the ring.

Because the protonated form of histidine is known to be a potent electron-transfer quencher of the indole chromophore,[79-81] we also investigated two interesting cases wherein a histidine resides in near contact with a Trp: Trp94, which is near His18 in barnase, and Trp138, which is near His105 in the Q105H/ W126Y/W158Y mutant of lyd. In the former, protonation of the His18 considerably lowers the quantum yield.[81] However, in the latter, protonation of His105 was unexpectedly found to increase the quantum yield.[82] For the Trp94-His18 pair in barnase, the lowest CT state is found to be on the ring of His18 most of the time and the energy of this CT state is quite low. For the W138-His105 pair in the lyd mutant, negative charges from several Asp and Glu residues near His105 apparently destabilize the His CT state and simultaneously stabilize the Trp amide CT state to the point that the lowest CT state is on the Trp amide. The Trp amide CT state is considerably destabilized by the presence of the protonated His18 next to the Trp ring, thereby increasing the Trp amide CT-^1L_a state gap, thereby increasing the quantum yield and fluorescence lifetime.

Effect of Protein and Water. The stabilization of the CT state by individual amino acid residues, waters, and ligands was estimated by a variation of the computer program that is used to add the electric potentials and fields due the protein/solvent

Feature Article

J. Phys. Chem. B, Vol. 108, No. 14, 2004 **4255**

environment to the QM Hamiltonian. The energy is estimated by the formula

$$\Delta E_{\text{env}} = \sum_{\alpha} V_{\alpha} \Delta \rho_{\alpha}$$

where V_{α} is the electric potential (in volts) at QM atom α and $\Delta\rho_{\alpha}$ is the change in electron density on atom α associated with the electron transfer. V_{α} is given by the Coulomb sum over all non-QM atoms by

$$V_{\alpha} = \sum_{k} q_k / r_{\alpha k}$$

with q_k the partial charge prescribed by the Charmm 26b force field for the kth non-QM atom and $r_{\alpha k}$ is the distance between the QM atom α and the non-QM atom k.

For Trp amides, the average total stabilization from protein and water varied from as much as 12 000 cm^{-1} (1.5 eV) for bpp and dsb126 to only 1000 cm^{-1} for stn and azb. The total stabilization correlates quite well with quantum yield, with the larger stabilization leading to small CT−^{1}L$_a$ energy gap and lower quantum yield.

For Trp amides, the range of stabilization by single residues extends from a maximum stabilization of about 8000 cm^{-1} (1 eV or 23 kcal/mol) for Arg77 of rnt to a maximum destabilization of 10 000 cm^{-1} by His$^+$18 of barnase and of 8000 cm^{-1} by Lys133 of stn. However, more typical magnitudes for maximum stabilization and destabilization by a single residue are about 5000 cm^{-1}. Single water molecules were found to stabilize by as much as 3000 cm^{-1} and to destabilize by as much as 1200 cm^{-1}.

The partitioning of stabilization between protein and water, however, was quite variable and did not correlate well with quantum yield. The range of total protein perturbation was from 15 500 cm^{-1} stabilization to as much as 12 500 cm^{-1} destabilization. The total water perturbation ran the range of 13 000 cm^{-1} stabilization to 5000 cm^{-1} of destabilization and was strongly anti-correlated with the protein stabilization. Thus, the net total stabilizations were not as extreme.

Discussion

We have benefited from previous QM−MM applications to electron transfer,[83−85] but this seems to be the first specific application to the quenching of Trp fluorescence by the amide and histidine systems. Indeed, this is the first attempt, to our knowledge, to predict quantum yields quantitatively for Trp fluorescence in unrelated proteins. However, the main purpose of this communication is not to present a particularly reliable quantitative procedure for predicting Trp fluorescence quantum yields but to present a comprehensive view of the several factors that must be involved and to articulate a promising new viewpoint. The idea is that local electric potential differences and solvent mobility are crucial in determining whether a particular group (usually a local amide) will be an effective quencher or not. Thus, the *location* of charged groups along the line connecting the Trp ring and electron acceptor will strongly influence the rate of electron transfer. For example, an aspartate group (or any negatively charged group) near the benzene ring end of Trp will lower the energy of the CT state and contribute to lowering the quantum yield. Replacing the aspartate with a neutral residue would likely increase the yield, giving the erroneous impression that aspartate was quenching by accepting an electron. Were the aspartate on the opposite side, near the amide, the opposite result would be expected.

Early Experiments. Cowgill[22] was perhaps the first to identify the variable fluorescence quantum yield of Trp and tyrosine (Tyr) as an interesting question. His early systematic study of Trp and Tyr derivatives clearly implicated the peptide bond as responsible for the generally low quantum yields in proteins. In addition, he drew attention to the high sensitivity of the yield to the electron withdrawing power of the group attached to the carbonyl, including the ability of protonated carboxylate and esters to quench. He also made the important observation that quenching by these groups did not occur in nonpolar solvents such as dioxane,[86,87] and this was later confirmed by Privat et al.[24] Steiner and Kirby[14] measured collisional quenching rate constants for amino acids and other related groups; they noted a strong correlation of the quenching and ability to scavenge hydrated electrons, thereby establishing a strong hypothesis that the quenching was related to electron transfer from the indole ring. Feitelson[23] confirmed much of Cowgill's findings and independently invoked electron transfer from the ring to amide, carboxylic acid, and ester groups, while at the same time recognizing proton-transfer quenching of the indole ring from ammonium, hydronium, etc., as a different process. He also confirmed Cowgill's assertion[88] that the simple amides (acetamide, and methyl acetamides) showed no measurable quenching effect as collisional quenchers.

Burstein and co-workers[8] studied the effect of collisional quenching by a number of small groups related to quenching in proteins, including amines, protonated amines, amides, thiols, and thiolate. They noted the ineffectiveness of amides as collisional quenchers and discovered the large deuterium isotope effect on the proton-transfer quenching by ammonium groups.

Ricci and Nesta[89] further established the validity of the electron transfer mechanism in their thorough study of quenching by carboxylic acids, esters and amides, clearly showing the correlation of quenching ability and electron withdrawing character of substituents on the carbonyl carbon.

Froehlich and Nelson[15] established a quantitative relation between the collisional quenching rate of substituted amides in aqueous solution and the pK_a of the corresponding carboxylic acid, further supporting the amide group as an electron acceptor in the quenching process. They also noted a substantial decrease in the quenching efficiency when the solvent was ethanol, noting that this was consistent with a charge-transfer mechanism.

A common thread in the early studies that greater electronegativity (carbonyl carbon more positive) of the substituent at the carbonyl resulted in lower quantum yields translates directly to our finding that more positive potential (charge) in the environment near the carbonyl leads to lower calculated quantum yield (because of a smaller CT-^{1}L$_a$ gap). In other words, there is no difference whether the positive charge is internal or external to the carbonyl-containing group.

Recent Studies. Petrich et al.[19] greatly strengthened the electron transfer quenching hypothesis in their steady state and time-resolved fluorescence study of three new model compounds: (3-indolylmethyl)malonamide (AA), diethyl (3-indolylmethyl)malonate (EE), and ethyl (3-indolylmethyl)malonate (AE) in which two amide, two ester, and one of each, respectively, are attached to the alpha carbon. With these and previously studied analogues, earlier work correlating electrophilicity of substituents was amplified, and a synergism was noted wherein the quenching rate caused by two substituents is far greater than additive. Temperature studies of the quenching rate revealed contrasting Arrhenius parameters for the temperature dependence of highly fluorescent indoles compared to the weakly fluorescent analogues bonded to electron acceptor

groups. Studies at low temperature and in viscous solvents showed that the puzzling single-exponential decay exhibited by NATA could not be because of fast interconversion on the fluorescence time scale.

The comprehensive study by Eftink et al.,[11] which included conformationally constrained Trp analogues, provided many new insights and provided an understanding of the synergistic effects involving proton-transfer quenching.

Two key studies from the Barkley group on the collisional quenching of 3MI in water carefully separated the effects of proton-transfer quenching by the ammonium group, intersystem crossing effects, and electron transfer to the amide[16] or other amino acid side chains.[13] The study by Chen et al.[16] demonstrated that electron transfer to amides is significant only when the collisional quenching unit contains two amides, with the effectiveness apparently increasing as the distance between the two amides decreases. This finding is consistent with the synergistic effects noted in earlier studies[11,19] and established the possibility that asparagine and glutamine residues in proteins could be significant quenchers. This work was then extended to other amino acids, also acylated to avoid quenching by the N-terminal ammonium group. They found that *protonated* glutamate and aspartate (by inference from protonated acetic acid), *protonated* histidine, and both the thiol and thiolate forms of cysteine all quench by electron transfer an order of magnitude more effectively than asparagine and glutamine, again in accord with earlier work on carboxylic acids and esters. The disulfide group has yet another order of magnitude higher collisional quenching rate constant.[15,19,89] The electron-transfer mechanism was inferred through isotope and temperature effects, as well as comparison of electron scavenging rates from the literature. On the other hand, the side chains of lysine and protonated tyrosine were found to quench by a proton-transfer mechanism. Because these studies were for collisional quenching of 3MI fluorescence in aqueous solution, they may be useful for qualitative predictions for Trps that are solvent exposed and more or less in contact with potential quenching groups. Given the reduced quenching in less polar solvents[24,86,87] and uncertainties regarding interaction and reorganization energy, extrapolating these results to Trps that are more buried is virtually impossible.

Engelborghs and co-workers[27,90] have carried out a particularly enlightening and provocative study of fluorescence lifetimes and quantum yields for Trp126 and Trp76 of the disulfide oxidoreductase DsbA from E. coli. The quantum yield of Trp126 is only 0.012. When the only two nearby quenching candidates, Asn127 and Gln74, were mutated to alanines, the quantum yield rose only to 0.04. No other reasonable candidates for electron transfer quencher residues exist for Trp126 besides the local backbone amide groups. This study strongly focuses attention to the local amide as the quenching group.

Nonexponential Fluorescence Decay: Rotamers. To this point, we have not mentioned a complicating detail, namely that in most cases the fluorescence decays nonexponentially. Many studies[19,20,25,91−95] have been directed at uncovering the cause of nonexponential fluorescence decay in model compounds, some of which is reviewed by Creed.[96] Beginning with the seminal work of Wahl and co-workers,[91] by far the dominant candidate has been the presence of multiple rotameric states that are noninterconverting on the fluorescence time scale. A reasonably self-consistent scheme emerged for Trp analogues and small Trp-containing peptides that includes distance and electrophilicity considerations.[19,94]

The scope of this paper, however, is to address the broad question of how a wide range of fluorescence quantum yields and lifetimes is observed for single Trp *proteins*, where the ubiquitous presence of multiple rotamers is more controversial. For this goal, a suitable working hypothesis has been to assume that the detailed local Trp rotamer conformation in *proteins* is given correctly by the published X-ray or NMR structures and that this rotamer is almost always the one with the major impact on the quantum yield in aqueous solution. At the other extreme is the approach exemplified by that of Engelborghs et al. in their interpretation of the nonexponential fluorescence decay from a number of proteins[28,30] that gives the X-ray structure assignment little weight compared to molecular modeling computational predictions of relative rotamer stability. By linking the effect of acrylamide quenching on lifetime decay components, electron-transfer rates were found to fit an exponential dependence on the distance from the Trp amide carbonyl C atom to the C4 (CE3) atom of the indole ring for Trp.[30] This is a remarkable result, given the delocalized nature of the indole electrons (Figure 2) and that other nearby amides are ignored.

Adams et al.[29] have recently combined fluorescence lifetime and NMR structural studies of a series of single-Trp hexapeptides designed to contain no quenching groups other than the peptide backbone. The quantum yields of Trp fluorescence from the hexapeptides were slightly higher than for NATA, but the decay required a three-exponent fit. In this study, 2-D NMR provided some evidence for different χ_1 rotamers being present. Some success was obtained in correlating electron transfer rates with rotamers, assuming that the rate depends exponentially on the distance of the center of the indole ring from the amide carbonyl carbon atoms, using a primitive orientation factor.

Recognizing that the protein environment may offer many more possibilities for nonexponential decay than a fixed set of rotamers, Bajzer and Prendergast[18] adapted theory originally applied to understanding nonexponential fluorescence decay arising from irreversible Förster transfer by a donor surrounded by randomly placed acceptors. In their approach, multiple lifetimes appear because of an assumed heterogeneity of active acceptors in the ensemble average. By invoking the possibility that not all potential quenchers are active for a given protein molecule at a given time, more observable decay constants are possible. This general approach is in harmony with the findings presented here, in that a given quencher can be active only when the resulting CT state is instantaneously isoenergetic with the fluorescing state. Indeed, we sometimes see cases during a trajectory when one, both, or neither of the two local amides are low in energy. Whether the persistence of such states is adequate to provide multiple lifetimes is unclear from our relatively short trajectories.

Ababou and Bombarda[26] have provided circumstantial evidence from measured temperature dependence of lifetime components for five proteins. Invoking the Bajzer−Prendergast approach,[18] they assumed that the short component was associated with ET to a nearby amide, but the long lifetime component was not. There was no explanation of why there would be two cases, however. If the environment of a Trp is the same for every Trp in the ensemble, then the two rates would be averaged and a single exponential would be observed. Their model would therefore require two substates, one wherein electron transfer could occur and another for which it could not occur.

Addressing the reversibility, Hudson et al.[17] point out that if the electron transfer to an unspecified acceptor is reversible, as would be the case when solvation of the CT state is not sufficient

Feature Article

J. Phys. Chem. B, Vol. 108, No. 14, 2004 **4257**

to permanently trap the charge separated state, the delayed return of the system to the fluorescing state formally leads to biexponential decay. Such a mechanism is clearly expected for those cases in Figures 3−5 for which the CT−^1L_a gap is small but the relaxation is also small.

Relative Importance of Electronic Coupling vs Reorganization and $\Delta G°$. A few comments are in order to contrast the present study with recent efforts to make sense of fluorescence lifetimes and quantum yields for single-Trp proteins in relation to electron transfer to nearby amides. Three of the studies above[28−30] have in common the assumption that the electron transfer rate depends exponentially on the distance between the donor indole ring and the acceptor amide carbon atom. This assumption comes from implicitly assuming that both the reorganization energy (λ) and $\Delta G°$ are the same for each rotamer, leaving the electronic coupling, V_{el}, as the only variable. Although both experiment and theory justify such an assumption for long range ET between systems that are very similar and in similar environments, it is highly questionable for short range (<5 Å) transfers between Trp and amides whose environments are different.

First we note that a number of studies of long-range electron transfer in proteins[31,32,97,98] and rigid glasses[99] suggest that if the electron-transfer process responsible for quenching of Trp fluorescence were activationless (meaning that $\Delta G° = -\lambda$), there would be significant quenching at distances as long as 12 Å. If extrapolated to the typical distances between the indole ring of Trp and the nearest amide (about 4−5 Å), ET rates of $\sim10^{12}$ s^{-1} are implied, over two orders above that required to reduce Trp fluorescence quantum yield to 0.01. Clearly, in the context of eq 5, the value of $|\Delta G° + \lambda|$ is large and small differences in this quantity will have large effects on the ET rate. Stated another way, small differences in the CT−^1L_a gap and/or the amplitude of fluctuations of this gap will have a profound effect when the gap is neither very small nor very large. For example, with a typical λ value of 1 eV and $\Delta G° = +0.5$ eV, the fractional increase in the Gaussian of eq 5 for a 0.1 eV (2.3 kcal/mol) reduction in $\Delta G°$ at 25 °C is 16-fold! This could account for a 10-fold difference in predicted lifetime or quantum yield. Given that the energy of a single hydrogen bond is about 5 kcal/mol, even the assumption that different Trp rotamers would have the same $|\Delta G° + \lambda|$ is not justified.

The extent to which *short-range* exponential distance dependence of electron transfer appears to be useful[26,28−30] is more likely linked strongly to the steep dependence of $\Delta G°$ on distance at short range because of the Coulomb attraction to be discussed next.

Long vs Short-Range Electron Transfer: Importance of Coulombic Interaction. Given that activationless long-range electron-transfer quenching of Trp fluorescence by transition metal ions had been demonstrated,[98] we were not necessarily expecting the local amide to be the primary acceptor. However, we found that the lowest CT state almost always involved a local electron transfer from the highest occupied molecular orbital (HOMO), localized on the Trp ring, to the nearest unoccupied backbone amide π^* MO. This is easily understood in terms of the Coulombic stabilization of the radical ion pair, a key ingredient in the famous Rehm−Weller equation. The CT state energy varies roughly as the reciprocal of the inter-ion distance. For example, the nearest amide is often on the order of only 4 Å from the ring. Increasing the donor−acceptor distance to 5 Å increases the energy of the CT state by about 0.7 eV (16 kcal/mol), if the transferred electron is concentrated at a point. Given the profound effect of only 0.1 eV noted above,

tempering this number with the effects of dielectric constant and delocalization of electron density in the donor, is unlikely to nullify the impact of distance on rate caused by Coulombic self-stabilization. If electron transfer is to be competitive with the intrinsic radiative and nonradiative rates of the 3MI chromophore, whose total is about 1.2×10^8 s^{-1}, the donor and acceptor must be close for activated electron transfer.

A number of works have explicitly omitted this important Coulombic term, often citing Miller et al.[99] Although it is true that the Born solvation would be quite reduced when the charge is spread over a large molecule, the Coulombic interaction of the separated charges at a distance of 10 Å is not much affected and is large. Even assuming a dielectric constant of 4, the interaction of unit charges separated by 10 Å is about 0.4 eV (8 kcal/mol). It is important to realize that Miller et al.[99] did not say that these effects were small and inconsequential. Indeed, they emphsized that they are quite important, changing $\Delta G°$ by ~0.5 eV. They did not include the correction because they did not know the dielectric constant of the glasses they were using and probably because it would not have changed the pattern of results and conclusions.

Relation of ΔE_{00} to Transition Energy Differences. The transition energies shown in Figures 3−6 are vertical energy differences between ground and ^1L_a or CT states at the CT minimum energy geometry. This geometry, characterized by much longer C=O and N−C amide bonds, considerably stabilizes the CT state while raising the energies of the ground and ^1L_a states. Therefore, if the Zindo transition energies are reasonably accurate, we expect to *add* about 3800 cm^{-1} (based on CASPT2 ground-state energies) to the transition energy difference to obtain an estimate of ΔE_{00}, the energy difference of the CT and ^1L_a states in their respective minimum energy geometries. That we need to *subtract* about 4000 cm^{-1} to obtain the fit in Figure 8 suggests either that the Zindo transition energies are considerably overestimated, i.e., that the TDDFT energies in Table 1 are more accurate or that the purely nonadiabatic treatment used here is not entirely appropriate. The formalism we have used says that most $^1L_a - $ CT energy level crossings do not lead to electron transfer because they occur too rapidly. However, if some of the crossings are slow enough to be in the adiabatic limit, wherein crossings become avoided crossings, the CT character in the "^1L_a" eigenstate increases as the environment fluctuation lowers the CT energy. When sufficient CT character has been acquired, the solvent response will become driven to further increase the CT character until a pure CT state is irreversibly reached. The latter process is much more efficient, requiring in principle only one such "crossing" during the lifetime of the excited state and, therefore, would not require the large FC overlap needed in the nonadiabatic theory, which we force by subtracting a large energy from the Zindo transition energy.

We are inclined to favor the latter explanation because the CASPT2 results (Table 1) suggest that the Zindo energies are underestimated. The general treatment of solvent assisted electron-transfer processes, such as the ones we include here, is difficult to implement without artificial separation of time scales.[77,100]

Future Work

First we remark that this study can be extended to the equally variable fluorescence yields and lifetimes observed for tyrosine in proteins. Virtually all behavior of Trp derivatives that points to electron transfer to the amides has a perfect parallel in the corresponding Tyr derivatives.[22,86,88,101] More generally, the

4258 *J. Phys. Chem. B, Vol. 108, No. 14, 2004*

Fluorescence Quantum Yields for Trp in Proteins

methods used here should be useful for studying other electron-transfer processes, e.g., those involving quenching of flavin fluorescence,[102,103] and fluorescent probes on DNA.

Future work will include an investigation of quenching by the disulfide group, which appears to be an effective quencher when within 6 Å.[90] The fluorescence lifetime for Trp69 in cutinase is 40 ps,[104] corresponding to a fluorescence quantum yield of about 0.002. There the disulfide bond is in direct contact with the Trp.

Yet another possible mechanism for Trp quenching must be considered. Nanda and Brand[105] and Subramaniam et al.[106] have discovered that a conserved Trp buried in a hydrophobic pocket containing mainly aromatic side chains in homedomain proteins uniformly exhibits a low fluorescence quantum yield. The cause of this is circumstantially linked to the low quantum yield and red-shifted fluorescence observed for indole in benzene. One member of this class has been investigated by us (d6o) and found to have a low predicted yield due to the local amide. We are planning simulations for other homeodomain proteins to see if this is a general property of the homeodomain Trp or if a phenomenon related to quenching by benzene is involved.[107,108]

We are also applying the method to a study of how electron-transfer quenching varies for different rotameric conformations. Preliminary results[109] show that indeed rotamer conformation can strongly affect fluorescence lifetime, *independent of the electronic coupling strength*. However, we intend to further refine our method by identifying more precisely how the electronic coupling depends on distance and orientation.

Finally, we note that the main principle here is independent of the exact nature of the CT state, leaving the possibility for $\pi\sigma^*$ type states that have recently come to light from high level quantum chemical computations.[110] A transition to this state would also entail a large dipole change, but toward the indole N–H bond instead of the amide. We are working on simulations that should help distinguish between these two possibilities.

Conclusion

The simulations presented here lead one to conclude that the full range of Trp fluorescence quantum yields (and lifetimes) observed in proteins is due primarily to different degrees of electron transfer from the indole ring to a local amide. The dependence on protein environment arises mainly from the average local electric potential difference between the Trp ring and local backbone amide and from the amplitude of potential difference variation caused by protein and solvent motions. This can be strongly influenced by the *location of nearby charges*. Negative (positive) charge will decrease (increase) the quantum yield if it is closer to the indole ring than to the electron acceptor because these arrangements stabilize (destabilize) the CT state. If the charge is closer to the acceptor, the opposite will be true.

Amides on other residues and good electron acceptors such as disulfide and histidine cation can be the primary quencher if the local electric potentials are favorable and if they are close enough. The extreme environmental sensitivity of the CT states allows for electron transfer when fluctuations invert the CT–^{1}L$_a$ energy gap, allowing for nonadiabatic or adiabatic electron transfer, followed by fast solvent relaxation about the CT state to create a low-lying, very weakly emitting solvent stabilized "radical ion pair". Trps satisfying both the narrow gap and large amplitude fluctuation/relaxation criteria are expected to exhibit low fluorescence quantum yields and short fluorescence lifetimes. A semiquantitative prediction using only the average energy gap and variance was achieved using only two adjustable parameters: a universal electronic coupling constant and a constant offset applied to the semiempirical transition energies. Closer acceptors are generally favored because the CT state is stabilized by donor–acceptor Coulombic interaction. Nonexponential fluorescence decay may be expected to arise naturally through various mechanisms in this view.

References and Notes

(1) Eftink, M. R. *Methods Biochem. Anal.* **1991**, *35*, 127–205.
(2) Meech, S. R.; Lee, A.; Phillips, D. *Chem. Phys.* **1983**, *80*, 317–28.
(3) Beechem, J. M.; Brand, L. *Annu. Rev.Biochem.* **1985**, *54*, 43–71.
(4) Demchenko, A. P. *Ultraviolet Spectroscopy of Proteins*; Springer-Verlag: New York, 1986; Vol. 1.
(5) Lakowicz, J. *Principles of Fluorescence Spectroscopy*, 2nd ed.; Plenum: New York, 1999.
(6) Ervin, J.; Sabelko, J.; Gruebele, M. *J. Photochem. Photobiol. B* **2000**, *54*, 1–15.
(7) Qiu, L.; Pabit, S. A.; Roitberg, A. E.; Hagen, S. J. *J. Am. Chem. Soc.* **2002**, *124*, 12952–3.
(8) Bushueva, T. L.; Busel, E. P.; Burstein, E. A. *Stud. Biophys.(Berlin)* **1975**, *52*, 41–52.
(9) Nakanishi, M.; Tsuboi, M. *Chem. Phys. Lett.* **1978**, *57*, 262–4.
(10) Shizuka, H.; Serizawa, M.; Kobayashi, H.; Kameta, K.; Sugiyama, H.; Matsuura, T.; Saito, I. *J. Am. Chem. Soc.* **1988**, *110*, 1726–32.
(11) Eftink, M. R.; Jia, Y.; Hu, D.; Ghiron, C. A. *J. Phys. Chem.* **1995**, *99*, 9, 5713–23.
(12) Yu, H. T.; Colucci, W. J.; McLaughlin, M. L.; Barkley, M. D. *J. Am. Chem. Soc.* **1992**, *114*, 8449–54.
(13) Chen, Y.; Barkley, M. D. *Biochemistry* **1998**, *37*, 9976–82.
(14) Steiner, R. F.; Kirby, E. P. *J. Phys. Chem.* **1969**, *73*, 4130–5.
(15) Froehlich, P. M.; Nelson, K. *J. Phys. Chem.* **1978**, *82*, 2401–3.
(16) Chen, Y.; Liu, B.; Yu, H.-T.; Barkley, M. D. *J. Am. Chem. Soc.* **1996**, *118*, 9271–8.
(17) Hudson, B. S.; Huston, J. M.; Soto-Campos, G. *J. Phys. Chem. A* **1999**, *103*, 2227–34.
(18) Bajzer, Z.; Prendergast, F. G. *Biophys. J.* **1993**, *65*, 2313–23.
(19) Petrich, J. W.; Chang, M. C.; McDonald, D. B.; Fleming, G. R. *J. Am. Chem. Soc.* **1983**, *105*, 3824–32.
(20) Chang, M. C.; Petrich, J. W.; McDonald, D. B.; Fleming, G. R. *J. Am. Chem. Soc.* **1983**, *105*, 3819–24.
(21) Bent, D. V.; Hayon, E. *J. Am. Chem. Soc.* **1975**, *97*, 2612–9.
(22) Cowgill, R. W. *Arch. Biochm. Biophys.* **1963**, *100*, 36–44.
(23) Feitelson, J. *Israel J. Chem.* **1970**, *8*, 241–52.
(24) Privat, J.-P.; Wahl, P.; Auchet, J.-C. *Biophys. Chem.* **1979**, *9*, 223–33.
(25) Colucci, W. J.; Tilstra, L.; Sattler, M. C.; Fronczek, F. R.; Barkley, M. D. *J. Am. Chem. Soc.* **1990**, *112*, 9182–90.
(26) Ababou, A.; Bombarda, E. *Protein Sci.* **2001**, *10*, 2102–13.
(27) Sillen, A.; Hennecke, J.; Roethlisberger, D.; Glockshuber, R.; Engelborghs, Y. *Proteins Struct., Funct., Genet.* **1999**, *37*, 253–63.
(28) Sillen, A.; Diaz, J. F.; Engelborghs, Y. *Protein Sci.* **2000**, *9*, 158–69.
(29) Adams, P. D.; Chen, Y.; Ma, K.; Zagorski, M. G.; Sonnichsen, F. D.; McLaughlin, M. L.; Barkley, M. D. *J. Am. Chem. Soc.* **2002**, *124*, 9278–86.
(30) Hellings, M.; DeMaeyer, M.; Verheyden, S.; Hao, Q.; VanDamme, E. J. M.; Peumans, W. J.; Engelborghs, Y. *Biophys. J.* **2003**, *85*, 1894–902.
(31) Beratan, D. N.; Betts, J. N.; Onuchic, J. N. *Science* **1991**, *252*, 1285–8.
(32) Gray, H. B.; Winkler, J. R. *Annu. Rev. Biochem.* **1996**, *65*, 561.
(33) Beratan, D. N.; Betts, J. N.; Onuchic, J. N. *J. Phys. Chem.* **1992**, *96*, 2852–955.
(34) Marcus, R. A. *J. Chem. Phys.* **1955**, *24*, 966–78.
(35) Tachiya, M. *J. Phys. Chem.* **1993**, *97*, 5911–6.
(36) Matyushov, D. V.; Voth, G. A. *J. Chem. Phys.* **2000**, *113*, 5413–24.
(37) Bixon, M.; Jortner, J. *Adv. Chem. Phys.* **1999**, *106*, 35–202.
(38) Vivian, J. T.; Callis, P. R. *Biophys. J.* **2001**, *80*, 2093–109.

Feature Article

J. Phys. Chem. B, Vol. 108, No. 14, 2004 **4259**

(39) Callis, P. R.; Burgess, B. K. *J. Phys. Chem.* **1997**, *101*, 9429−32.

(40) Callis, P. R.; Vivian, J. T. *Chem. Phys. Lett.* **2003**, *369*, 409−14.

(41) Ridley, J.; Zerner, M. *Theor. Chim. Acta (Berlin)* **1973**, *32*, 111−34.

(42) Theiste, D.; Callis, P. R.; Woody, R. W. *J. Am. Chem. Soc.* **1991**, *113*, 3, 3260−7.

(43) Sreerama, N.; Woody, R. W.; Callis, P. R. *J. Phys. Chem.* **1994**, *98*, 10397−407.

(44) Li, J.; Williams, B.; Cramer, C. J.; Truhlar, D. G. *J. Phys. Chem.* **1999**, *110*, 724−33.

(45) MacKerell, A. D., Jr.; Bashford, D.; Bellott, M.; et al. *J. Phys. Chem. B* **1998**, *102*, 3586−616.

(46) Ryckaert, J. P.; Cicotti, G.; Berendsen, H. J. C. *J. Comput. Phys.* **1977**, *23*, 327−41.

(47) Short, K. W.; Callis, P. R. *J. Chem. Phys.* **2000**, *113*, 5235−44.

(48) Fender, B. J.; Short, K. W.; Hahn, D. K.; Callis, P. R. *Int. J. Quantum Chem.* **1998**.

(49) Callis, P. R.; Vivian, J. T.; Slater, L. S. *Chem. Phys. Lett.* **1995**, *244*, 53−8.

(50) Frisch, M. J.; Trucks, G. W.; Schlegel, H. B.; Scuseria, G. E.; Robb, M. A.; Cheeseman, J. R.; Zakrzewski, V. G.; Montgomery, J. A., Jr.; Stratmann, R. E.; Burant, J. C.; Dapprich, S.; Millam, J. M.; Daniels, A. D.; Kudin, K. N.; Strain, M. C.; Farkas, O.; Tomasi, J.; Barone, V.; Cossi, M.; Cammi, R.; Mennucci, B.; Pomelli, C.; Adamo, C.; Clifford, S.; Ochterski, J.; Petersson, G. A.; Ayala, P. Y.; Cui, Q.; Morokuma, K.; Malick, D. K.; Rabuck, A. D.; Raghavachari, K.; Foresman, J. B.; Cioslowski, J.; Ortiz, J. V.; Stefanov, B. B.; Liu, G.; Liashenko, A.; Piskorz, P.; Komaromi, I.; Gomperts, R.; Martin, R. L.; Fox, D. J.; Keith, T.; Al-Laham, M. A.; Peng, C. Y.; Nanayakkara, A.; Gonzalez, C.; Challacombe, M.; Gill, P. M. W.; Johnson, B. G.; Chen, W.; Wong, M. W.; Andres, J. L.; Head-Gordon, M.; Replogle, E. S.; Pople, J. A. *Gaussian 98*, revision A.11.3; Gaussian, Inc.: Pittsburgh, PA, 1998.

(51) MOLCAS5.4 Andersson, K.; Barysz, M.; Bernhardsson, A.; Blomberg, M. R. A.; Cooper, D. L.; Fülscher, M. P.; de Graaf, C.; Hess, B. A.; Karlström, G.; Lindh, R.; Malmqvist, P.-Å.; Nakajima, T.; Neogrády, P.; Olsen, J.; Roos, B. O.; Schimmelpfennig, B.; Schütz, M.; Seijo, L.; Serrano-Andrés, L.; Siegbahn, P. E. M.; Stålring, J.; Thorsteinsson, T.; Veryazov, V.; Widmark, P.-O. Lund University: Lund, Sweden, 2002.

(52) Serrano-Andres, L.; Roos, B. O. *J. Am. Chem. Soc.* **1996**, *118*, 185−95.

(53) Serrano-Andres, L.; Fulscher, M. P. *J. Am. Chem. Soc.* **1998**, *120*, 10912−20.

(54) Callis, P. R. *Int. J. Quantum. Chem.* **1984**, *S18*, 579−88.

(55) Callis, P. R. *J. Chem. Phys.* **1991**, *95*, 4230−40.

(56) Rehms, A. A.; Callis, P. R. *Chem. Phys. Lett.* **1987**, *140*, 83−9.

(57) Callis, P. R.; Rehms, A. A. *Chem. Phys. Lett.* **1993**, *208*, 276−82.

(58) Eftink, M. R.; Selvidge, L. A.; Callis, P. R.; Rehms, A. A. *J. Phys. Chem.* **1990**, *94*, 3469−79.

(59) Sammeth, D. M.; Siewert, S. S.; Spangler, L. H.; Callis, P. R. *Chem. Phys. Lett.* **1992**, *193*, 532−8.

(60) Sammeth, D. M.; Yan, S.; Spangler, L. H.; Callis, P. R. *J. Phys. Chem.* **1990**, *94*, 7340−2.

(61) Fender, B. J.; Sammeth, D. M.; Callis, P. R. *Chem. Phys. Lett.* **1995**, *239*, 31−7.

(62) Fender, B. J.; Callis, P. R. *Chem. Phys. Lett.* **1996**, *262*, 343−8.

(63) Callis, P. R. *Methods Enzymol.* **1997**, *278*, 113−50.

(64) Muino, P. L.; Callis, P. R. *J. Chem. Phys.* **1994**, *100*, 4093−109.

(65) Ilich, P.; Haydock, C.; Prendergast, F. G. *Chem. Phys. Lett.* **1989**, *158*, 129−34.

(66) Simonson, T.; Wong, C. F.; Bruenger, A. T. *J. Phys. Chem. A* **1997**, *101*, 1935−45.

(67) Strickland, E. H.; Horwitz, J.; Billups, C. *Biochemistry* **1970**, *9*, 4914−20.

(68) Bickel, G. A.; Demmer, D. R.; Outhouse, E. A.; Wallace, S. C. *J. Chem. Phys.* **1989**, *91*, 6013−9.

(69) Sobolewski, A.; Domcke, W. *Phys. Chem.* **2003**.

(70) Loring, R. A. *J. Phys. Chem.* **1990**, *94*, 513−5.

(71) Jimenez, R.; Fleming, G. R.; Kumar, P. V.; Maroncelli, M. *Nature* **1994**, *369*, 471−3.

(72) Hopfield, J. J. *Proc. Natl. Acad. Sci, U.S.A.* **1974**, *71*, 3640−4.

(73) Fõrster, Th. *Discuss. Faraday Soc* **1959**, *27*, 7.

(74) Fõrster, Th. *Chem. Phys. Lett.* **1971**, *12*, 422−4.

(75) Kestner, N. R.; Logan, J.; Jortner, J. *J. Phys. Chem.* **1974**, *78*, 2148−66.

(76) Marcus, R. A.; Sutin, N. *Biochim. Biophys. Acta* **1985**, *811*, 265−322.

(77) Barzykin, A. V.; Frantsuzov, P. A.; Seki, K.; Tachiya, M. *Adv. Chem. Phys.* **2002**, *123*, 511−616.

(78) Daizadeh, I.; Medvedev, E. S.; Stuchebrukhov, A. A. *Proc. Natl. Acad. Sci, U.S.A.* **2003**, *94*, 3703−8.

(79) Shinitzky, M.; Fridkin, M. *Eur. J. Biochem.* **1969**, *9*, 176−81.

(80) Bushueva, T. L.; Busel, E. P.; Bushuev, V. N.; Burstein, E. A. *Stud. Biophys. (Berlin)* **1974**, *44*, 129−39.

(81) De-Beuckeleer, K.; Volckaert, G.; Engelborghs, Y. *Proteins* **1999**, *36*, 42−53.

(82) Van Gilst, M.; Hudson, B. S. *Biophys. Chem.* **1996**, *63*, 17−25.

(83) Warshel, A. *J. Phys. Chem.* **1982**, *86*, 2218−24.

(84) Carter, E.; Hynes, J. T. *J. Chem. Phys.* **1991**, *94*, 5961−79.

(85) Gehlen, J. N.; Marchi, M.; Chandler, D. *Science* **1994**, *263*, 499−502.

(86) Cowgill, R. W. *Biochim. Biophys. Acta* **1967**, *133*, 6−18.

(87) Muino, P. L. Callis, P. R. Solvent effects on fluorescence quantum yields of tryptophan derivatives. Manuscript in preparation, 2004.

(88) Cowgill, R. W. *Biochim. Biophys. Acta* **1970**, *200*, 18−25.

(89) Ricci, R. W.; Nesta, J. M. *J. Phys. Chem.* **1976**, *80*, 974−80.

(90) Hennecke, J.; Sillen, A.; Huber, W. M.; Engelborghs, Y. *Biochemistry* **1997**, *36*, 6391−400.

(91) Donzel, B.; Gaudechon, P.; Wahl, P. *J. Am. Chem. Soc.* **1974**, *96*, 801−8.

(92) Fleming, G. R.; Morris, J. M.; Robbins, R. J.; Woolfe, G. J.; Thistlethwaite, P. J.; Robinson, G. W. *Proc. Natl. Acad. Sci. U.S.A.* **1978**, *75*, 4652−6.

(93) Szabo, A. G.; Rayner, D. M. *J. Am. Chem. Soc.* **1980**, *102*, 554−63.

(94) Engh, R. A.; Chen, L. X. Q.; Fleming, G. R. *Chem. Phys. Lett.* **1986**, *126*, 365−72.

(95) Dahms, T. E. S.; Willis, K. J.; Szabo, A. G. *J. Am. Chem. Soc.* **1995**, *117*, 2321−6.

(96) Creed, D. *Photochem. Photobiol.* **1984**, *39*, 537−62.

(97) Petrich, J. W.; Longworth, J. W.; Fleming, G. R. *Biochemistry* **1987**, *26*, 2711−34.

(98) Supkowski, R. M.; Bolender, J. P.; Smith, W. D.; Reynolds, L. E. L.; Horrocks, W. D. *Coord. Chem. Rev.* **1999**, *185*, 307−19.

(99) Miller, J. R.; Peeples, J. A.; Schmitt, M. J.; Closs, G. L. *J. Am. Chem. Soc.* **1982**, *104*, 6488−93.

(100) Cho, M.; Fleming, G. R. *Adv. Chem. Phys.* **1999**, *107*, 311−70.

(101) Lukomska, J.; Rzeska, A.; Malicka, J.; Wiczk, W. *J. Photochem. Photobiol. A: Chem.* **2001**, *143*, 135−9.

(102) Mataga, N.; Chosrowjan, H.; Shibata, Y.; Tanaka, F.; Nishina, Y.; Shiga, K. *J. Phys. Chem. B* **2000**, *104*, 10667−77.

(103) Yang, H.; Luo, G.; Karnchanaphanurach, P.; Louie, T.-M.; Rech, I.; Cova, S.; Xun, L.; Xie, X. S. *Science* **2003**, *302*, 262−6.

(104) Weisenborn, P. C. M.; Meder, H.; Egmond, M. R.; Visser, T. J. W. G.; van Hoek, A. *Biophys. Chem.* **1996**, *58*, 281−8.

(105) Nanda, V.; Liang, S. M.; Brand, L. *Biochem. Biophys. Res. Commun.* **2000**, *279*, 770−8.

(106) Subramaniam, V.; Jovin, T. M.; Rivera-Pomar, R. V. *J. Biol. Chem.* **2001**, *276*, 21506−11.

(107) Suwaiyan, A.; Klein, U. K. A. *Chem. Phys. Lett.* **1989**, *159*, 244−50.

(108) Van Duuren, B. L. *J. Org. Chem.* **1961**, *26*, 2954−60.

(109) Muino, P. L. Callis, P. R. *Biophys. J.* **2003**, *84*, 289a.

(110) Sobolewski, A. L.; Domcke, W.; Dedonder-Lardeux, C.; Jouvet, C. *Phys. Chem. Chem. Phys.* **2002**, *2*, 1093−100.

(111) Harris, D. L.; Hudson, B. S. *Chem. Phys.* **1991**, *158*, 353−82.

(112) Gastmans, M.; Volckaert, G.; Engelborghs, Y. *Proteins June* **1999**, *35*, 464−74.

(113) Egan, D. A.; Logan, T. M.; Liang, H.; Matayoshi, E.; Fesik, S. W.; Holzman, T. F. *Biochemistry* **1993**, *32*, 1920−7.